Croatian Society for Materials Protection

Metalurgija/Metallurgy

Vol. 66 No. 2 / 2027

Study on Wear-Resistant Heat Treatment Process of Pole Tips for Outdoor Mountaineering Poles

Li Zhan [1,*] and Yanli Jiang [2]

https://doi.org/10.64486/m.66.2.2

1 Harbin University, Harbin City, No. 109 Zhongxing Avenue, Nangang District, Heilongjiang Province, China, 150086
2 Shenzhen Polytechnic University, Shenzhen City, No. 4089, West Shahe Road, Nanshan District, Guangdong Province, China, 518055; jylzhl@163.com
* Correspondence: zhanli@hrbu.edu.cn

Type of the Paper: Article
Received: May 19, 2026
Accepted: July 17, 2026

Abstract: Outdoor mountaineering pole tips are small but safety-critical components because they directly contact ice, snow, wet rock and other complex terrains. Their service stability depends on both the load-bearing capacity of the steel substrate and the antifriction/wear resistance of the copper alloy working layer. In this study, 42CrMo/ZCuPb10Sn10 Fe/Cu bimetallic pole tips were prepared by solid-liquid compound casting followed by an integrated casting-heat treatment route. The work focuses on how quenching temperature and holding time affect interfacial bonding, microstructure evolution, Pb-particle distribution, hardness and dry-sliding wear behavior. The results indicate that heat treatment improves the interfacial shear strength and microhardness compared with the as-cast state. When the quenching temperature is 850 °C and the holding time is further optimized to 90 min, the interdiffusion distance, interfacial shear strength and wear resistance reach the best overall combination among the investigated conditions. One-way ANOVA confirmed significant effects of the heat-treatment condition on interfacial shear strength, friction coefficient and wear rate ($p < 0.01$). SEM/EDS observations and quantitative indicators suggest that this improvement is associated with a finer Cu-side structure near the interface, reduced Sn segregation and a more dispersed Pb phase that may contribute to friction reduction during sliding. The conclusions are discussed as a process-microstructure-property relationship for Fe/Cu bimetallic pole tips within the range of the presented experimental evidence.

Keywords: outdoor mountaineering pole tips; Fe/Cu bimetal; 42CrMo/ZCuPb10Sn10; integrated casting-heat treatment; interfacial bonding; friction and wear

1. Introduction

In recent years, the safety and service reliability of outdoor mountaineering equipment have attracted increasing attention because mountaineering, rock climbing and ice climbing are often performed on complex terrains where slipping and impact injuries may occur [1]. For pole tips used on ice, snow, wet rock and gravel surfaces, the working end repeatedly experiences impact, sliding friction and local stress concentration. Ice-friction studies also show that interfacial sliding behavior is sensitive to contact conditions, surface state and test method [2]. Therefore, the pole tip requires not only sufficient strength but also stable interfacial bonding and wear resistance during repeated anti-skid service. Steel/copper bimetallic structures are suitable for such components because the steel side can provide load-bearing capacity, whereas the copper-alloy side can provide antifriction and wear-resistant functionality [3], [4]. In the present work, 42CrMo steel and ZCuPb10Sn10 leaded tin bronze were selected to form a Fe/Cu bimetallic pole-tip material. Solid-liquid compound casting is an efficient route for preparing bimetallic parts with metallurgical bonding [5]. However, Fe and Cu have limited mutual solubility, and the as-cast interface may contain insufficient diffusion, local defects and weak bonding. In addition, the copper layer may exhibit dendritic segregation, Pb-particle agglomeration and Sn-rich regions, all of which can affect hardness, friction behavior and wear stability.

Heat treatment is an important approach for regulating interfacial diffusion, residual stress and microstructural uniformity in bimetallic materials. Jiang et al. reported that heat treatment changed the reaction layer and bonding strength of compound-cast aluminum/steel bimetals [6]. Ho et al. showed that continuous cooling heat treatment affected the interface characteristics of S45C/copper compound castings [7], while Bina et al. observed that heat treatment modified the bonding interface of explosive-welded copper/stainless-steel composites [8]. Recent research on aluminum-bronze/steel bimetallic structures also indicates that post-heat treatment can homogenize the bronze-side microstructure and reduce residual stress [9]. These studies demonstrate that thermal processing can improve bimetallic interfaces, but they also suggest that the temperature and holding-time window must be controlled carefully. For Fe/Cu bimetals containing leaded tin bronze, the copper-layer response is especially important. First-principles calculations have shown that Ni, Sn and P can influence the adhesion electronic properties of gamma-Fe/Cu heterogeneous interfaces [10]. In Cu-Sn alloys and Pb-Sn bronzes, Sn distribution, Pb morphology and hard phosphide phases are closely related to strength, hardness and tribological behavior [11], [12]. Studies on ZCuPb20Sn5 alloy and leaded brass further indicate that the distribution of soft lead-rich phases and surface morphology can influence friction reduction and wear response [13], [14]. Therefore, the wear behavior of 42CrMo/ZCuPb10Sn10 pole tips should be discussed together with interfacial diffusion, Pb-particle morphology, Sn segregation and hard-phase evolution.

Although the above studies provide useful guidance, most of them focus on plates, cylinders, welded joints or additively manufactured bimetals rather than small special-shaped pole-tip components prepared by an integrated casting-heat treatment route. Moreover, quenching temperature and holding time are often discussed separately, while their combined influence on interfacial bonding and wear behavior remains important for service parts. The effect of temperature on microstructure and sliding wear has also been reported for wear-resistant steels [15], which further supports the need to link thermal parameters with wear performance in the present bimetallic system. Recent studies have further strengthened the process-structure-property framework for steel/copper and tin-bronze systems. Wan et al. deposited a CuPb10Sn10 antifriction layer on 42CrMo steel and reported reliable interfacial bonding together with reduced friction [16]. Chen et al. showed that subsequent heat treatment can promote elemental homogenization and improve the interfacial mechanical performance of steel/CuSn10 bimetallic structures [17], while Liu et al. demonstrated that copper/steel bimetals produced by CMT-WAAM exhibit process-dependent interfacial microstructures and hardness gradients [18]. For cast Cu-Sn-based alloys, Shi et al. linked the morphology and distribution of soft phases to mechanical and tribological performance [19]. More directly, recent studies on 42CrMo/CuPb10Sn10 and Cu-10Pb-10Sn/steel bimetals have quantified the relationships among grain refinement, Fe/Cu interdiffusion, shear strength, friction coefficient and wear rate under different processing and sliding conditions [20], [21]. These findings provide a recent basis for evaluating the combined effects of heat-treatment temperature and holding time in the present solid-liquid compound-cast system.

In this study, 42CrMo/ZCuPb10Sn10 bimetallic pole tips for outdoor mountaineering poles were prepared by solid-liquid compound casting followed by integrated heat treatment. The effects of quenching temperature and holding time on interfacial microstructure, microhardness, shear strength and friction/wear behavior were investigated. By combining SEM/EDS observations, diffusion-distance analysis, Pb-particle statistics and wear indicators, this work aims to establish a process-microstructure-property relationship and to identify a heat-

 https://doi.org/10.64486/m.66.2.2

treatment condition that improves interfacial bonding and wear resistance without departing from the actual pole-tip application background.

2. Materials and Methods

2.1. Experimental Materials and Substrate Pretreatment

Fe/Cu bimetallic pole-tip samples were prepared by a solid-liquid compound casting process. 42CrMo steel was selected as the solid substrate to provide structural strength, and ZCuPb10Sn10 copper alloy was used as the liquid wear-resistant layer to provide antifriction and wear-resistant functionality. The chemical compositions of the two materials are shown in Table 1. The purity of all metal raw materials was ≥99.9 %, and phosphorus was added in the form of phosphorus-copper master alloy (14 wt. %).

Table 1. Chemical composition of experimental materials (wt. %)

Material	C	Si	Mn	Cr	Mo	Pb	Sn	Zn	Ni	P	Fe	Cu
42CrMo steel	0.45	0.37	0.80	1.20	0.25	-	-	-	-	≤0.03	Balance	-
ZCuPb10Sn10	-	-	-	-	-	9–11	9–11	1.7	2	0.05–0.1	-	Balance

The preparation process was divided into the following three steps:

- Surface treatment of steel matrix: The 42CrMo steel matrix was ultrasonically cleaned with NaOH (8 %–12 %) aqueous solution and HCl (10 %–15 %) aqueous solution for 15 min in sequence to remove oil and oxide film, then rinsed with anhydrous ethanol, dried with cold air, and coated with high-temperature anti-oxidation coating.
- Copper alloy melting: The copper alloy was melted in a pit resistance furnace at 1200 °C ± 20 °C. Pure copper, pure nickel, alloying elements and phosphorus-copper master alloy were added in sequence, stirred evenly and held for 30 min.
- Composite casting and integrated heat treatment: The molten copper alloy was poured into the preheated 42CrMo steel matrix mold. When the solidification temperature decreased to the preset quenching temperature, the casting was transferred into a heat-treatment furnace for holding, then cooled to room temperature by oil quenching, and finally tempered at 500 °C for 120 min to reduce residual stress.

Five quenching-temperature conditions were designed at a fixed holding time of 60 min (750 °C, 800 °C, 850 °C, 900 °C and 950 °C). After determining 850 °C as the preferred quenching temperature, five holding-time conditions were further considered at 850 °C (30 min, 60 min, 90 min, 120 min and 150 min). The full process matrix is shown in Table 2.

Table 2. Heat treatment process parameters of Fe/Cu bimetallic pole tips

Material grade	Heat treatment process	Quenching	Quenching	Holding
42CrMo/ZCuPb10Sn10	As-cast	-	-	-
	Quenching + Tempering	mechanical oil	750	60
	Quenching + Tempering	mechanical oil	800	60
	Quenching + Tempering	mechanical oil	850	60
	Quenching + Tempering	mechanical oil	900	60

https://doi.org/10.64486/m.66.2.2

Material grade	Heat treatment process	Quenching	Quenching	Holding
	Quenching + Tempering	mechanical oil	950	60
42CrMo/ZCuPb10Sn10	Quenching + Tempering	mechanical oil	850	30
42CrMo/ZCuPb10Sn10	Quenching + Tempering	mechanical oil	850	90
42CrMo/ZCuPb10Sn10	Quenching + Tempering	mechanical oil	850	120
42CrMo/ZCuPb10Sn10	Quenching + Tempering	mechanical oil	850	150

2.2. Experimental Equipment and Test Methods

2.2.1. Main Experimental Equipment

The core equipment used in the experiment included: an SG2-12-12 box-type crucible resistance furnace and a matching tempering furnace, a differential scanning calorimeter for thermal analysis, a TUKON-2100B Vickers hardness tester, a WDW-20/30 universal electronic mechanical testing machine, a Zeiss metallographic microscope, an SU5000 field emission scanning electron microscope equipped with energy-dispersive spectroscopy (SEM/EDS), an ER230 3D topography measuring profilometer and an MRH-3A high-speed ring-block wear testing machine.

2.2.2. Microstructure Characterization

Metallographic samples were cut from the pole tip samples by wire cutting machine, ground step by step with 240#-2000# silicon carbide sandpaper, polished and then etched. The steel side was etched with 4 % nitric acid alcohol solution for (5–7) s, and the copper side was etched with a mixed solution of ammonia water: hydrogen peroxide: water = 1:1:3 for (90–120) s.

The interface and copper-layer microstructures were observed by metallographic microscopy and SEM. Element distributions were analyzed by EDS point, line and mapping analyses. The size and distribution of Pb particles were counted using ImageJ from micrographs obtained under the same magnification; these data were used as quantitative support for the discussion of Pb refinement and agglomeration.

2.2.3. Performance Test

- Interfacial shear strength test: The interfacial shear strength of the Fe/Cu bimetal was tested on a WDW-20/30 universal electronic mechanical testing machine with a loading rate of 1 mm/min. Each condition was tested three times in parallel, and the results are reported as mean ± SD.
- Microhardness test: The microhardness of the Fe/Cu bimetal interface was measured by a TUKON-2100B Vickers hardness tester with a test load of HV0.05 and a holding time of 10 s. One test point was set every 50 μm along the direction perpendicular to the interface, with the interface as the coordinate origin. Each data point was obtained from the average of five measurements around the selected position.
- Friction and wear performance test: The friction and wear test was carried out on an MRH-3A high-speed ring-block wear testing machine with a ring-block contact friction pair. The sample was cut by wire cutting, and the copper layer working surface was ground to 2000# mesh, polished, rinsed with anhydrous ethanol and dried with cold air. Both the sample and the counterpart ring were ultrasonically cleaned with acetone for (8–10) min and dried before the test.

The test was carried out at room temperature under dry-friction conditions with a rotating speed of 200 r/min, test load of 50 N and friction time of 30 min. Each group of friction tests was repeated three times, and the friction coefficient and wear rate were reported as mean ± SD. The worn-surface morphology and wear debris were observed by SEM/EDS. Wear-rate and 3D worn-profile data were used together with SEM/BSE observations so that the wear mechanism was not inferred from morphology alone. Shear-strength, friction-coefficient and wear-rate results are reported as mean ± SD from three independent tests, while microhardness

https://doi.org/10.64486/m.66.2.2

values are based on multiple indentation measurements as described above. The discussion focuses on trends consistently supported by several measurements rather than on marginal numerical differences.

2.2.4. Statistical Analysis

Interfacial shear strength, friction coefficient and wear rate are expressed as mean ± standard deviation (SD) from three independent tests (n = 3). The quenching-temperature series (as-cast, 750 °C, 800 °C, 850 °C, 900 °C and 950 °C) and holding-time series (30 min, 60 min, 90 min, 120 min and 150 min at 850 °C) were analyzed separately by one-way analysis of variance (ANOVA), followed by Tukey's post hoc test for multiple comparisons. Differences were considered statistically significant at $p < 0.05$. The Fe/Cu interdiffusion distance, EDS point-composition data and worn-profile parameters were treated as descriptive microstructural or topographical indicators. Error bars in Figure 2(b) represent SD (n = 3).

3. Results and Discussion

3.1. Effect of Quenching Temperature on Microstructure of the Material

Quenching temperature is the core parameter of heat treatment process, which directly determines the atomic diffusion kinetic energy, grain size evolution and phase transformation process, and thus regulates the macroscopic properties of the bimetal. In this section, based on the DSC analysis results of as-cast ZCuPb10Sn10 alloy, the quenching temperature range was determined, and the regulation law of quenching temperature on the interfacial microstructure, mechanical properties and friction and wear properties of Fe/Cu bimetal was systematically investigated.

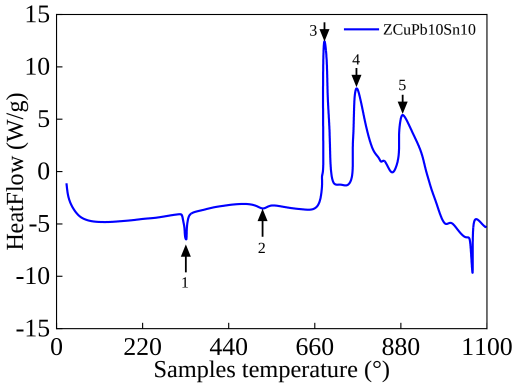

Figure 1. DSC curve of as-cast ZCuPb10Sn10 alloy

Figure 1 shows the heating DSC curve of as-cast ZCuPb10Sn10 alloy. The test was carried out from room temperature 25 °C to 1100 °C with a heating rate of 10 °C/min under argon protection. It can be seen from Figure 1 that an exothermic peak exists at position (1), corresponding to the temperature range of 321 °C–337 °C, which is highly consistent with the theoretical crystallization temperature of Pb (327.46 °C), so it is determined as the phase transformation peak of Pb phase. A weak exothermic peak at position (2) corresponds to the temperature range of 510 °C–536 °C, which is determined as the eutectoid reaction peak at 520 °C combined with the Cu-Sn binary alloy phase diagram. An endothermic peak at position (3) corresponds to the temperature range of 656 °C–701 °C, which is the eutectoid reaction peak of Cu-Sn alloy. The endothermic peak at position (4) corresponds to the temperature range of 745 °C–826 °C, with the peak temperature of the precipitation interval at 767 °C, which is the peritectic reaction peak of the alloy. The endothermic peak at position (5) corresponds to the precipitation interval of α-Cu phase.

The setting of heat treatment temperature for Fe/Cu bimetal must take into account the microstructure transformation characteristics of both steel side and copper side. 42CrMo steel is a hypoeutectoid steel, and its conventional quenching temperature is 30 °C–50 °C above the Ac3 line. According to the DSC test results, ZCuPb10Sn10 alloy has a peritectic reaction in the range of 745 °C–826 °C with a peak temperature of 767 °C, and the tin bronze has a wide crystallization temperature range. Based on the above factors, 5 quenching

 https://doi.org/10.64486/m.66.2.2

temperature gradients (750 °C, 800 °C, 850 °C, 900 °C, 950 °C) were set in this experiment with 750 °C as the starting point and 50 °C as the gradient.

3.2. Effect of Quenching Temperature on Interfacial Shear Strength of the Material

Figure 2 and Table 3 show the interfacial shear response of the Fe/Cu bimetal at different quenching temperatures. The as-cast sample has a shear strength of 200.6 MPa. After heat treatment, the shear strength increases and then decreases with increasing quenching temperature, reaching 233.6 MPa at 850 °C. This trend is consistent with the EDS diffusion-distance results, which show that the interdiffusion distance increases from 6.74 μm in the as-cast state to 10.78 μm at 850 °C. Therefore, the improvement in shear strength is discussed as being associated with enhanced interfacial diffusion and a more favorable interfacial microstructure rather than with hardness change alone. When the quenching temperature is 750 °C and 800 °C the interfacial shear strength increases to 223.4 MPa and 231.2 MPa, respectively. At these temperatures, heat treatment promotes atomic interdiffusion near the interface and reduces the degree of segregation in the copper side. When the quenching temperature rises to 850 °C the interface shows the best bonding among the investigated conditions. Further increasing the temperature to 900 °C and 950 °C reduces the shear strength to 225.2 MPa and 223.1 MPa, respectively. This decrease is consistent with the observed coarsening tendency of the copper-side structure and the tendency of Pb particles to agglomerate, both of which may introduce local stress concentration. The statement is therefore interpreted as a structure-assisted bonding effect supported by SEM/EDS observations and diffusion-distance measurements.

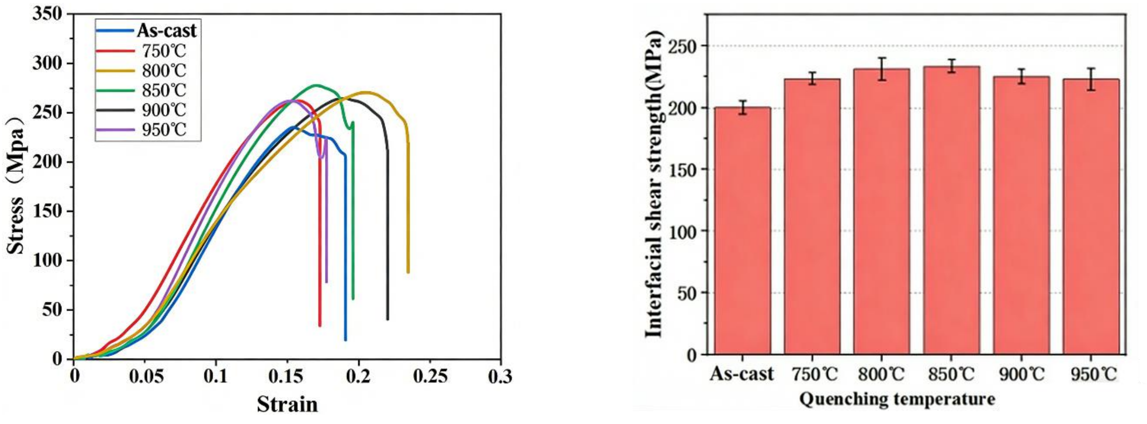

(a) Stress-strain curves (b) Interfacial shear strength

Figure 2. Interfacial shear response of Fe/Cu bimetal at different quenching temperatures (Error bars in panel (b) represent SD, n = 3).

3.3. Microhardness Analysis

Figure 3 shows the microhardness distribution on both sides of the Fe/Cu interface at different quenching temperatures. The average microhardness of the as-cast steel side and copper side is 271.7 HV and 91.2 HV, respectively. Heat treatment increases the hardness of both sides. For the copper layer, the improvement is mainly related to reduced Sn segregation and possible solid-solution strengthening of α-Cu, as indicated by the EDS results listed in Table 4. For the steel side, the transformation from ferrite/pearlite to tempered sorbite after quenching and tempering contributes to the higher hardness.

The hardness increase should be interpreted together with the wear data. According to Archard-type wear behavior, a higher matrix hardness generally reduces the wear rate under comparable sliding conditions, but the Pb distribution and possible transfer-film formation also play roles in leaded bronze. Thus, the improved wear resistance at 850 °C is discussed as the combined result of hardness improvement, reduced Sn segregation and a more favorable Pb-particle distribution, rather than as the consequence of a single factor.

When the quenching temperature is 750 °C the average microhardness of the steel side is 331.8 HV and that of the copper side is 98.2 HV. At 850 °C the corresponding values reach 352.2 HV and 107.6 HV, which are

https://doi.org/10.64486/m.66.2.2

29.63 % and 17.98 % higher than those of the as-cast state, respectively. When the temperature is further increased to 950 °C the hardness changes only slightly (351.4 HV on the steel side and 108.2 HV on the copper side), indicating that the additional temperature increase no longer improves the overall structure-property balance.

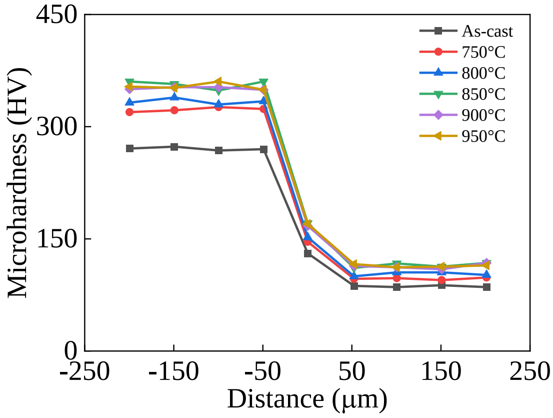

Figure 3. Microhardness distribution curves of Fe/Cu bimetal interface at different quenching temperatures

3.4. Wear Morphology and Wear Mechanism Analysis

Figure 4 shows the SEM and BSE morphology of the worn surface of the Fe/Cu bimetal copper layer treated at different quenching temperatures under dry-friction conditions. The images were compared under the same magnification, and the SEM and BSE image sequence and corresponding scale bars are identified in the figure caption. In the as-cast sample, deep ploughing grooves and adhesive spalling pits indicate severe material removal. This observation is consistent with the highest friction coefficient (0.4903) and wear rate (3.523×10^{-7} $mm^3/(N{\cdot}m)$) listed in Table 3.

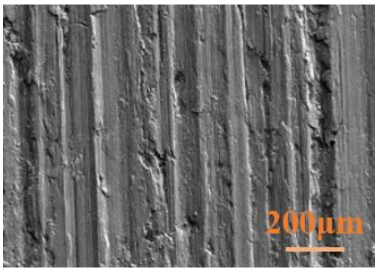

(a) As-cast - SEM image

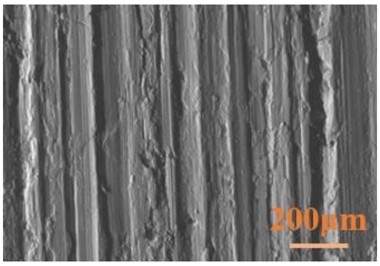

(b) As-cast - BSE image

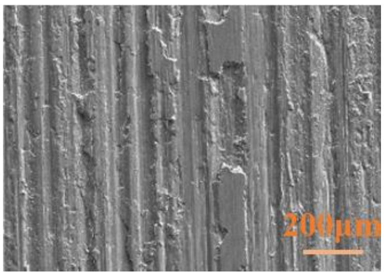

(c) 750 °C quenched - SEM image

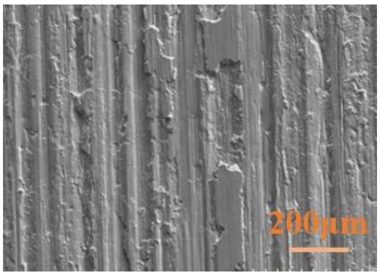

(d) 750 °C quenched - BSE image

https://doi.org/10.64486/m.66.2.2

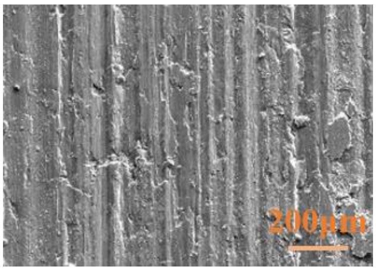

(e) 800 °C quenched - SEM image

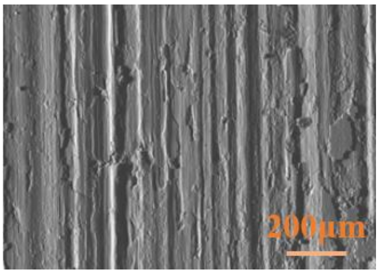

(f) 800 °C quenched - BSE image

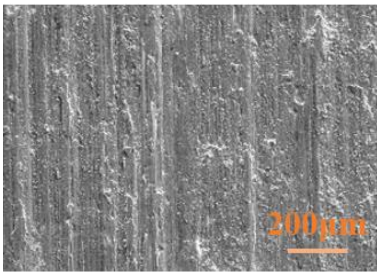

(g) 850 °C quenched - SEM image

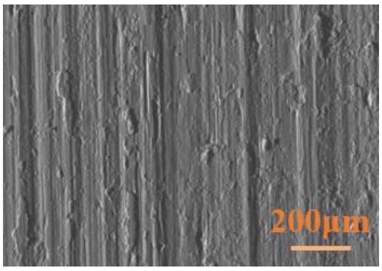

(h) 850 °C quenched - BSE image

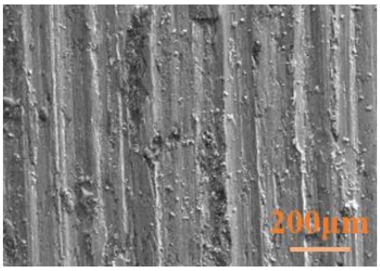

(i) 900 °C quenched - SEM image

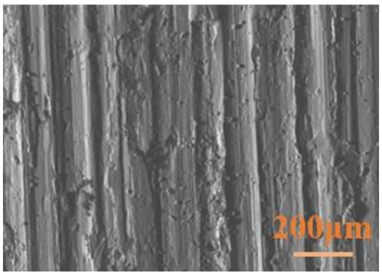

(j) 900 °C quenched - BSE image

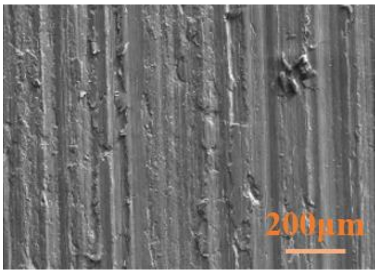

(k) 950 °C quenched - SEM image

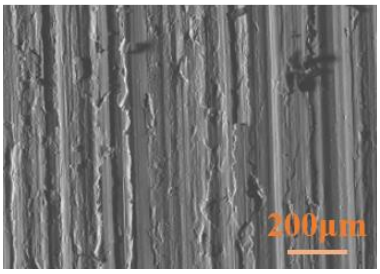

(l) 950 °C quenched - BSE image

Figure 4. SEM and BSE morphology of the worn surface of Fe/Cu bimetal copper layer at different quenching temperatures

At 750 °C and 800 °C the worn surface contains fewer delamination areas and shallower ploughing grooves than the as-cast surface. The friction coefficient decreases to 0.4136 and 0.3219, and the wear rate decreases to 2.856×10^{-7} $mm^3/(N \cdot m)$ and 2.331×10^{-7} $mm^3/(N \cdot m)$, respectively. At 850 °C, the worn surface is comparatively smooth, with only slight scratches. This corresponds to the lowest friction coefficient and wear rate in the quenching-temperature series. The mechanism is interpreted as mild abrasive wear, possibly accompanied by Pb-related friction reduction, as supported by the EDS mapping results and quantitative wear indicators rather than by morphology alone. When the quenching temperature increases to 900 °C and 950 °C scratches and grooves reappear and powdery wear debris is observed. The friction coefficient and wear rate also increase. These results suggest that excessive temperature weakens the beneficial microstructural refinement and may

https://doi.org/10.64486/m.66.2.2

promote Pb-particle coarsening/agglomeration. Therefore, the wear-resistance deterioration at high temperature is discussed as a combined effect of structural coarsening and a less favorable Pb-particle distribution.

Figures 5 and 6 show the elemental mapping results of the worn surfaces of the as-cast and 850 °C quenched samples, respectively. In the as-cast sample, Pb is present as relatively coarse agglomerates and does not form a continuous lubricating layer. Sn-rich regions correspond to δ-Cu-Sn phase, while the co-enrichment of P and Ni indicates Ni3P. These harder phases can locally support the load, but the uneven Pb and Sn distributions still lead to unstable friction. The detection of Fe on the worn surface is attributed to transfer from the 45# steel counterpart ring during sliding. For the 850 °C sample, fine Pb particles are more uniformly distributed in the wear track. During sliding, these particles may be extruded and transferred to the contact surface, reducing direct metal-to-metal contact. This explanation is supported by the lower friction coefficient, lower wear rate, EDS mapping and the Pb-particle statistics summarized below. Therefore, Pb-related lubrication is considered a likely contributor to the improved wear behavior rather than the sole wear mechanism.

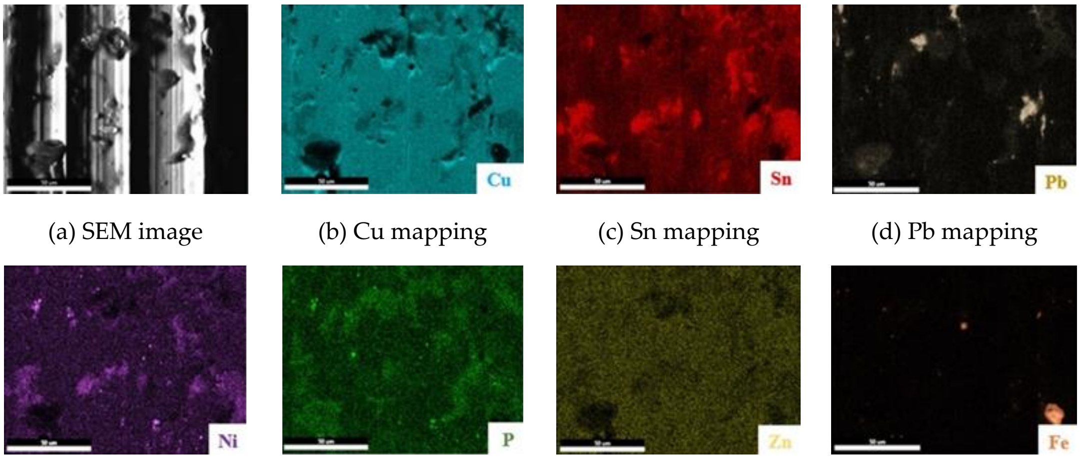

(a) SEM image (b) Cu mapping (c) Sn mapping (d) Pb mapping

(e) Ni mapping (f) P mapping (g) Zn mapping (h) Fe mapping

Figure 5. Elemental mapping of the worn surface of as-cast Fe/Cu bimetal copper layer

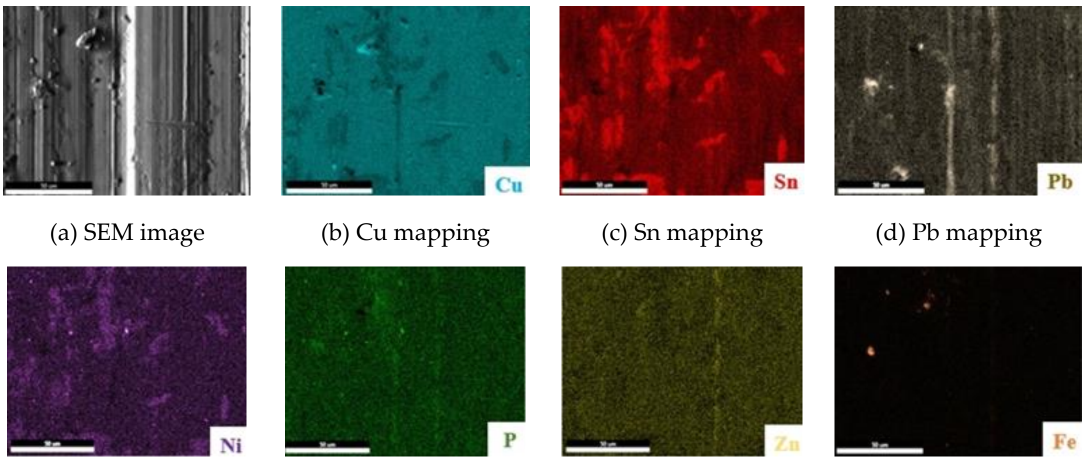

(a) SEM image (b) Cu mapping (c) Sn mapping (d) Pb mapping

(e) Ni mapping (f) P mapping (g) Zn mapping (h) Fe mapping

Figure 6. Elemental mapping of the worn surface of 850 °C quenched Fe/Cu bimetal copper layer

https://doi.org/10.64486/m.66.2.2

3.5. Quantitative Composition and Pb-Particle Analysis

To strengthen the quantitative microstructural support, the mechanism discussion is limited to the evidence presented in the text: SEM/BSE morphology, EDS mapping, EDS point analysis, diffusion-distance measurements and ImageJ particle statistics. These results indicate that heat treatment mainly improves the structure-property balance by refining the copper-side morphology, reducing Sn segregation and dispersing Pb particles. Accordingly, the discussion avoids treating phase evolution or grain-boundary behavior as independent proof for the conclusions.

The interfacial diffusion-distance data provide direct support for the bonding discussion. Compared with the as-cast state, heat treatment increases the measured Fe/Cu interdiffusion distance up to 850 ℃, which is consistent with the increase in interfacial shear strength. The decrease at 900 °C–950 °C indicates that higher temperature is not necessarily beneficial, most likely because structural coarsening and Pb agglomeration counteract the benefit of diffusion. Therefore, the interpretation is supported by the presented SEM/EDS observations and mechanical test results.

Table 3. Quantitative indicators at different quenching temperatures

Condition	Fe/Cu interdiffusion distance / µm	Interfacial shear strength / MPa	Friction coefficient	Wear rate / (10^{-7} mm^3/(N·m))
As-cast	6.74	200.6 ± 6.0	0.4903 ± 0.0255	3.523 ± 0.173
750 ℃ / 60 min	8.61	223.4 ± 6.9	0.4136 ± 0.0194	2.856 ± 0.151
800 ℃ / 60 min	9.34	231.2 ± 7.9	0.3219 ± 0.0167	2.331 ± 0.117
850 ℃ / 60 min	10.78	233.6 ± 6.3	0.2461 ± 0.0118	1.937 ± 0.101
900 ℃ / 60 min	9.93	225.2 ± 6.8	0.3094 ± 0.0158	2.226 ± 0.109
950 ℃ / 60 min	7.25	223.1 ± 7.4	0.3318 ± 0.0159	2.349 ± 0.117

Note: Interfacial shear strength, friction coefficient and wear rate are presented as mean ± SD (n = 3). Interdiffusion distance is used as a descriptive EDS line-scan indicator.

The quantitative data show that the 850 °C, 60 min condition gives the best performance in the quenching-temperature series. The interdiffusion distance and shear strength increase by approximately 59.9 % and 16.5 %, respectively, compared with the as-cast state, while the friction coefficient and wear rate decrease by approximately 49.8 % and 45.0 %. Because the changes are consistent across bonding and wear indicators, the selected quenching temperature is supported by multiple datasets. Minor numerical differences are not overinterpreted because the reported values are used mainly to identify the overall process trend. One-way ANOVA showed significant effects of quenching-temperature condition on interfacial shear strength ($F(5,12) = 8.62$, $p = 0.001$), friction coefficient ($F(5,12) = 68.90$, $p < 0.001$) and wear rate ($F(5,12) = 56.66$, $p < 0.001$). Tukey's test showed that all heat-treated groups had significantly higher shear strength than the as-cast group, whereas the differences among the heat-treated groups were not significant. The 850 °C group had a significantly lower friction coefficient than all other groups and a significantly lower wear rate than the as-cast, 750 °C, 800 °C and 950 °C groups; its wear rate did not differ significantly from that at 900 °C.

https://doi.org/10.64486/m.66.2.2

Table 4. EDS-based Sn segregation analysis in the copper layer at different quenching temperatures

Condition	Sn in dendrite core, point 1 / at.%	Sn in interdendritic region, point 2 / at.%	Difference at. %	Interpretation
As-cast	3.59	12.47	8.88	Severe Sn segregation
750 °C	4.66	10.89	6.23	Segregation reduced
800 °C	5.33	10.50	5.17	Segregation reduced
850 °C	7.31	8.43	1.12	Best Sn homogenization
900 °C	6.25	8.20	1.95	Moderate homogenization
950 °C	6.46	8.64	2.18	Slight coarsening tendency

ImageJ particle counting further supports the Pb-refinement discussion. In the 850 °C sample, the numbers of Pb particles in the (0–10) μm^2 and (10–50) μm^2 size intervals are 406 and 192, respectively, while large Pb particles above 50 μm^2 are greatly reduced. This statistical trend provides quantitative support for the observed dispersion of the Pb phase after heat treatment. At higher temperatures, the reappearance of coarse/agglomerated Pb is consistent with the increased friction coefficient and wear rate, but the Pb effect is treated as one contributor rather than the only cause of the wear behavior.

3.6. Effect of Holding Time on Interfacial Bonding and Wear Behavior

At 850 °C, a short holding time of 30 min is insufficient for interfacial diffusion and may leave small defects near the interface. Extending the holding time to (60–90) min improves diffusion and bonding. When the holding time is further increased to (120–150) min, the interdiffusion distance and shear strength decrease, which is attributed to Cu-side grain coarsening and a reduced number of effective diffusion channels.

Table 5. Quantitative indicators at different holding times under 850 °C quenching

Holding time min	Fe/Cu interdiffusion distance / μm	Interfacial shear strength / MPa	Friction coefficient	Wear rate / (10^{-7} $mm^3/(N{\cdot}m)$)
30	5.47	176.3 ± 8.6	0.3936 ± 0.0192	2.513 ± 0.122
60	10.78	233.6 ± 6.3	0.2461 ± 0.0118	1.937 ± 0.101
90	12.35	248.9 ± 12.2	0.2278 ± 0.0116	1.813 ± 0.091
120	8.97	231.4 ± 12.0	0.2421 ± 0.0114	1.902 ± 0.101
150	8.32	209.4 ± 10.1	0.2584 ± 0.0132	2.094 ± 0.103

Note: Interfacial shear strength, friction coefficient and wear rate are presented as mean ± SD (n = 3). Interdiffusion distance is used as a descriptive EDS line-scan indicator.

The 90 min holding time gives the maximum interdiffusion distance and interfacial shear strength. Relative to the 60 min condition, the shear strength increases from (233.6 ± 6.3) MPa to (248.9 ± 12.2) MPa, while the friction coefficient decreases from 0.2461 ± 0.0118 to 0.2278 ± 0.0116 and the wear rate decreases from (1.937 ± 0.101) × 10^{-7} $mm^3/(N{\cdot}m)$ to (1.813 ± 0.091) × 10^{-7} $mm^3/(N{\cdot}m)$. These consistent changes justify revising the preferred process from 850 °C, 60 min to 850 °C, 90 min within the investigated process range. One-way ANOVA confirmed significant holding-time effects on interfacial shear strength ($F(4,10) = 19.47$, $p < 0.001$), friction coefficient ($F(4,10) = 73.20$, $p < 0.001$) and wear rate ($F(4,10) = 21.26$, $p < 0.001$). Tukey's test showed that the 90 min group had significantly higher shear strength than the 30 min and 150 min groups and a significantly

https://doi.org/10.64486/m.66.2.2

lower wear rate than those two groups. The friction coefficient at 30 min was significantly higher than at all longer holding times, whereas the differences among (60–150) min were not significant.

Table 6. Worn-profile parameters at different holding times

Holding time / min	Maximum valley depth / μm	Worn profile area / μm²
30	105.06	322490
60	90.63	253076
90	79.30	183090
120	88.39	246109
150	97.65	264623

The worn-profile parameters provide additional evidence for the tribological interpretation. The smallest valley depth and worn area occur at 90 min, matching the lowest friction coefficient and wear rate. Therefore, the improved wear behavior is attributed to the combined effects of increased hardness, reduced Sn segregation and possible Pb-assisted friction reduction, rather than to Pb-film formation alone.

EDS analysis of Sn distribution also supports the holding-time effect. At 30 min, the Sn difference between the dendrite core and interdendritic region is about 10.18 at. %, indicating significant segregation. At 90 min, this difference decreases to about 0.44 at. %, showing that Sn is more uniformly distributed in the α-Cu matrix. At 150 min, the Sn distribution remains relatively uniform, but the bonding and wear advantages decrease, which is consistent with structural coarsening and Pb agglomeration. Thus, a longer holding time is not necessarily better.

4. Conclusions

In this paper, 42CrMo/ZCuPb10Sn10 bimetallic pole tips for outdoor mountaineering poles were taken as the research object. An integrated casting-heat treatment process was used to investigate the effects of quenching temperature and holding time on interfacial bonding, microstructure, hardness and dry-sliding wear behavior. The main conclusions are as follows:

1. Quenching temperature regulates interfacial diffusion, hardness and wear resistance of 42CrMo/ZCuPb10Sn10 bimetal. As the temperature increases from 750 °C to 850 °C the interdiffusion distance, shear strength and wear resistance improve; further increasing the temperature to 900 °C–950 °C leads to a decline in bonding and wear behavior. This trend is consistent with the competition between beneficial diffusion/microstructural refinement and excessive structural coarsening/Pb agglomeration.
2. At a fixed holding time of 60 min, the best quenching temperature is 850 °C. Under this condition, the interdiffusion distance reaches 10.78 μm, the interfacial shear strength reaches 233.6 MPa, the steel-side and copper-side average microhardness values reach 352.2 HV and 107.6 HV, respectively, the friction coefficient decreases to 0.2461 and the wear rate decreases to 1.937×10^{-7} $mm^3/(N \cdot m)$.
3. Holding time further optimizes the integrated heat-treatment process. At 850 °C the 90 min holding condition gives the best comprehensive performance, with an interdiffusion distance of 12.35 μm, interfacial shear strength of 248.9 MPa, friction coefficient of 0.2278 and wear rate of 1.813×10^{-7} $mm^3/(N \cdot m)$. Excessive holding time reduces the interdiffusion distance and shear strength, which is consistent with Cu-side structural coarsening and Pb-particle agglomeration observed in the microstructural analysis.
4. SEM/EDS observations, Sn-segregation analysis and Pb-particle statistics indicate that the optimized process improves the copper-side structure and promotes a more favorable distribution of Sn and Pb. The wear mechanism changes from severe adhesive/abrasive wear in the as-cast state to milder abrasive

https://doi.org/10.64486/m.66.2.2

wear after the optimized heat treatment, with Pb-related friction reduction considered as a contributing mechanism. Therefore, oil quenching at 850 °C for 90 min followed by tempering at 500 °C for 120 min is selected as the preferred process for the investigated Fe/Cu bimetallic pole tips.

References

[1] V. Schöffl, A. Morrison, I. Schöffl, and T. Küpper, "The Epidemiology of Injury in Mountaineering, Rock and Ice Climbing," in Epidemiology of Injury in Adventure and Extreme Sports, T. W. Heggie and D. J. Caine, Eds. Basel, Switzerland: S. Karger, 2012, vol. 58, pp. 17–43, https://doi.org/10.1159/000338575

[2] E. Jansons, J. Lungevics, I. Velkavrh, and T. Wright, "Ice friction: A Brief Review of the Influencing Factors and Experimental Methods," Friction, vol. 13, no. 9, Art. no. 9441076, 2025. https://doi.org/10.26599/FRICT.2025.9441076

[3] S. Kammerloher, J. Hoyer, P. Lechner, T. Mittler, and W. Volk, "A Method for Characterising the Influence of Casting Parameters on the Metallurgical Bonding of Copper and Steel Bimetals," Materials, vol. 14, no. 20, Art. no. 6223, 2021. https://doi.org/10.3390/ma14206223

[4] X. Fang, Y. Yin, S. Huang, M. Xu, J. Miao, and R. Li, "Study on Effects of Cooling Process on Mechanical and Tribological Properties of Melt-Casting Copper–Steel Bimetallic Composites," Materials Science, vol. 30, no. 3, pp. 310–318, 2024. https://doi.org/10.5755/j02.ms.36016

[5] W. Jiang, Z. Fan, and C. Li, "Improved Steel/Aluminum Bonding in Bimetallic Castings by a Compound Casting Process," Journal of Materials Processing Technology, vol. 226, pp. 25–31, 2015. https://doi.org/10.1016/j.jmatprotec.2015.06.032

[6] W. Jiang, G. Li, Y. Wu, X. Liu, and Z. Fan, "Effect of Heat Treatment on Bonding Strength of Aluminum/Steel Bimetal Produced by a Compound Casting," Journal of Materials Processing Technology, vol. 258, pp. 239–250, 2018. https://doi.org/10.1016/j.jmatprotec.2018.04.006

[7] J.-S. Ho, C. B. Lin, and C. H. Liu, "Effect of Continuous Cooling Heat Treatment on Interface Characteristics of S45C/Copper Compound Casting," Journal of Materials Science, vol. 39, no. 7, pp. 2473–2480, 2004. https://doi.org/10.1023/B:JMSC.0000020012.88809.33

[8] M. H. Bina, F. Dehghani, and M. Salimi, "Effect of heat treatment on bonding interface in explosive welded copper/stainless steel," Materials & Design, vol. 45, pp. 504-509, 2013, https://doi.org/10.1016/j.matdes.2012.09.037.

[9] J. Liu, Y. Miao, Z. Wang, Y. Zhao, Y. Wu, and C. Li, "Effect of Heat Treatment on Microstructure and Properties of Additively Manufactured Aluminum Bronze–Steel Bimetallic Structures," Materials Characterization, vol. 207, Art. no. 113462, 2024. https://doi.org/10.1016/j.matchar.2023.113462

[10] M. Wang, H. Han, G. Zhang, H. Xu, Z. Yin, Y. Dong, and Y. Fu, "Effect of Solute Elements (Ni, Sn, P) on the Adhesion Electronic Properties of γ-Fe/Cu Heterogeneous Interface: A First-Principles Study," Results in Physics, vol. 38, Art. no. 105659, 2022. https://doi.org/10.1016/j.rinp.2022.105659

[11] M. Karthik, J. Abhinav, and K. V. Shankar, "Morphological and Mechanical Behaviour of Cu–Sn Alloys: A Review," Metals and Materials International, vol. 27, no. 7, pp. 1915–1946, 2021. https://doi.org/10.1007/s12540-020-00899-z

[12] X. Ren, Z. Shi, G. Zhang, N. Chen, Y. Zhang, Z. Guo, J. Hu, and H. Xu, "Strengthening Mechanism of Sub-Nano Ni3P and Cu3P Phases Particles on the Pb–Sn Bronze Alloy," Heliyon, vol. 10, no. 15, Art. no. e34624, 2024. https://doi.org/10.1016/j.heliyon.2024.e34624

[13] X. Ren, G. Zhang, H. Xu, F. Sun, Y. Kang, M. Wang, J. Niu, C. Xu, and W. Lv, "Wear Resistance of ZCuPb20Sn5 Alloy," Tribology, vol. 40, no. 4, pp. 467–476, 2020. https://doi.org/10.16078/j.tribology.2019161 (in Chinese)

[14] J. Huang, Y. Guan, and S. Ramakrishna, "Tribological Behavior of Femtosecond Laser-Textured Leaded Brass," Tribology International, vol. 162, Art. no. 107115, 2021. https://doi.org/10.1016/j.triboint.2021.107115

[15] C. Li, X. Deng, L. Huang, Y. Jia, and Z. Wang, "Effect of Temperature on Microstructure, Properties and Sliding Wear

Behavior of Low Alloy Wear-Resistant Martensitic Steel," Wear, vols. 442–443, Art. no. 203125, 2020. https://doi.org/10.1016/j.wear.2019.203125

[16] L. Wan, M. Cheng, G. Fu, C. Wei, T. Shi, and S. Shi, "Annular laser cladding of CuPb10Sn10 copper alloy for high-quality anti-friction coating on 42CrMo steel surface," Optics & Laser Technology, vol. 158, Art. no. 108878, 2023, https://doi.org/10.1016/j.optlastec.2022.108878

[17] J. Chen, G. Bi, D. Zhao, D. Wang, M. Zhang, and Y. Xiao, "Subsequent enhancement of mechanical properties using heat treatment of steel/copper bimetallic structures manufactured by laser powder bed fusion," Journal of Materials Research and Technology, vol. 33, pp. 8944-8957, 2024, https://doi.org/10.1016/j.jmrt.2024.11.213

[18] Y. Liu, B. Li, W. Zhang, Z. Liu, and M. Jiang, "Interfacial behavior of copper/steel bimetallic composites fabricated by CMT-WAMM," Coatings, vol. 14, no. 7, Art. no. 803, 2024, https://doi.org/10.3390/coatings14070803

[19] Z. Shi, H. Xu, G. Zhang, Y. Liu, and X. Ren, "Effect of Bi content on the microstructure, mechanical and tribological properties of Cu-Sn alloy," Materials, vol. 16, no. 20, Art. no. 6658, 2023, https://doi.org/10.3390/ma16206658

[20] Z. Shi, Y. Zhang, G. Zhang, H. Xu, and X. Ren, "Effect of electromagnetic stirring current on the microstructure, mechanical and tribological properties of copper/steel bimetal," Materials Today Communications, vol. 47, Art. no. 113126, 2025, https://doi.org/10.1016/j.mtcomm.2025.113126

[21] Y. Zhang, Z. Shi, G. Zhang, X. Ren, and H. Xu, "Tribological behavior of Cu-10Pb-10Sn/steel bimetals under different loads and speeds: Dry, kerosene, and oil lubrication conditions," Journal of Materials Engineering and Performance, vol. 35, no. 2, pp. 1171-1183, 2026, https://doi.org/10.1007/s11665-025-11620-9